

AD-A216 625

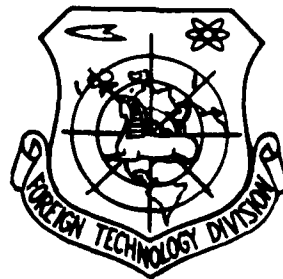
FOREIGN TECHNOLOGY DIVISION



A DIFFERENCE SCHEME WITH AUTOCONTROL ARTIFICIAL VISCOSITY TO PREDICT
ABLATED NOSETIP SHAPE

by

Yang Maozhao



DTIC
ELECTE
JAN 10 1990
S E D
M

Approved for public release;
Distribution unlimited.



90 01 10 110

HUMAN TRANSLATION

FTD-ID(RS)T-0640-89 29 September 1989

MICROFICHE NR: FTD-89-C-000800

A DIFFERENCE SCHEME WITH AUTOCONTROL ARTIFICIAL
VISCOSITY TO PREDICT ABLATED NOSETIP SHAPE

By: Yang Maozhao

English pages: 10

Source: Yuhang Xuebao, Nr. 3, 1988, pp. 55-60

Country of origin: China

Translated by: SCITRAN

F33657-84-D-0165

Requester: FTD/TQTAV/Jeffery D. Locker

Approved for public release; Distribution unlimited.

THIS TRANSLATION IS A RENDITION OF THE ORIGINAL FOREIGN TEXT WITHOUT ANY ANALYTICAL OR EDITORIAL COMMENT STATEMENTS OR THEORIES ADVOCATED OR IMPLIED ARE THOSE OF THE SOURCE AND DO NOT NECESSARILY REFLECT THE POSITION OR OPINION OF THE FOREIGN TECHNOLOGY DIVISION

PREPARED BY:

TRANSLATION DIVISION
FOREIGN TECHNOLOGY DIVISION
WPAFB, OHIO.



GRAPHICS DISCLAIMER

All figures, graphics, tables, equations, etc. merged into this translation were extracted from the best quality copy available.

Accession For	
NTIS GRA&I	<input checked="" type="checkbox"/>
DTIC TAB	<input checked="" type="checkbox"/>
Unannounced	<input type="checkbox"/>
Justification	
By _____	
Distribution/ _____	
Availability Codes	
Dist	Avail and/or Special
A-1	

A DIFFERENCE SCHEME WITH AUTOCONTROL ARTIFICIAL VISCOSITY
TO PREDICT ABLATED NOSETIP SHAPE

Yang Maozhao

(China Aerodynamic Research and Development Centre)

Abstract: The trio-layer explicit difference scheme which is added artificial viscosity item is found by using filtration in the computation of ablated nosetip shape. The scheme is of first order accuracy in regions where shape change is wavy and second order accuracy in regions where is Smooth. Numerical experiments show that the scheme developed is effective.

Subject Terms: Ablative nose cone, Reentry heating, Aerodynamic shape, Finite difference theory, *Keywords: Translations, China, (language) foreign technology*

1. Introduction

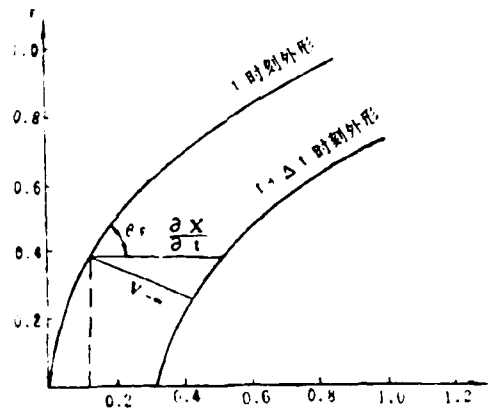
During reentry the aerodynamic heating is very strong in region of missile nosetip where the ablative rate of surface area is very large causing great shape change. The prediction of ablated nosetip shape has thus been a crucial problem in ablative coupling calculation. Some people have used eigen linear methods to solve shape equations and obtained the dispersion data of shape versus time [1]. The data have then been processed by three sampling smoothing and finally given the tip shape at each calculation time. Other people have solved shape equations by immediate application

Received on November 17, 1986.

of difference theory [2]. To remove the data fluctuation in calculations, they added artificial viscosity item to difference schemes appropriately. These methods have been successful in region where shape change is not great. However, in case some ablated shapes such as deep hollow and long nose cone happen, these calculations may become difficult or may lack accuracy at some specific points. In order to solve this problem, we, inspired by the shock wave data processing [4], have tried auto filtration of shape parameters in calculation of ablated reentry nosetip shape, found a trio-layer explicit difference scheme, solved shape equations by difference theory and successfully calculated the types of shapes with deep hollow and long nose cone. Numerical experiments have showed that this scheme is effective in guaranting required calculation accuracy as well as enlarging time steps. It has also been proved that this scheme is of first order accuracy in regions where shape change is wavy and it is of second order accuracy in region where shape change is Smooth.

2. Difference Scheme with Autocontrol Artificial Viscosity for Shape Prediction

Figure 1 shows the coordinate system (x, r) to which a missile is tied where the two curves represent nosetip shapes at time t and $t+\Delta t$, respectively, and the surface inclination is $\text{tg } \theta_F = \frac{\partial r(x,t)}{\partial x}$. Let $V_{-\infty}$ be the ablative velocity along the surface, it is easy to derive the deforming velocity of shape along x direction from Figure 1 which is



KEY: 1--shape at time t; 2-- shape at time t + Δt

Figure 1 Coordinate system for shape calculation

$$\frac{\partial x}{\partial t} = V_{-\infty} / \sin \theta_F$$

or in other words the differential equation for ablated nosetip shape can be written in the form of

$$\frac{\partial x}{\partial t} = V_{-\infty} \sqrt{1 + \left(\frac{\partial x}{\partial r}\right)^2} \quad (1)$$

Taking the derivative of (1) with respect to r gives the differential equation for velocity of surface inclination change. Let $y = \frac{\partial x}{\partial r} = \text{ctg } \theta_F$

we get

$$\frac{\partial y}{\partial t} = \sqrt{1+y^2} \left(V_{-\infty} \frac{y}{1+y^2} \frac{\partial y}{\partial r} + \frac{\partial V_{-\infty}}{\partial r} \right) \quad (2)$$

(1) and (2) constitute a set of nonlinear partial differential equations which can be solved by developing some difference scheme. After that shape parameters are smoothed by three sampling techniques. Our paper introduces a trio-layer explicit difference scheme with

autocontrol artificial viscosity item. Combining (1) and (2) as a set, we solved it by difference theory without the need of three sampling evening up. For that, first partially linearize equation (2). Let

$$\zeta = \sqrt{1 + \left(\frac{\partial x}{\partial r}\right)^2} = \sqrt{1 + y^2}$$

$$\alpha = V_{-\infty} \zeta$$

$$\beta = \frac{\partial V_{-\infty}}{\partial r} \cdot \zeta$$

$$A = V_{-\infty} y / \zeta$$

Equations (1) and (2) then become

$$\frac{\partial x}{\partial t} = \alpha \tag{3}$$

$$\frac{\partial y}{\partial t} = A \frac{\partial y}{\partial r} + \beta \tag{4}$$

Assuming that α , β and A are temporarily fixed, (3) and (4) then become linear equations. Following paper [4] to induce filtration function Q , the equations can be solved by developing trio-layer explicit difference schemes. That is,

$$\frac{x_j^{n+1} - [(1-Q_1)x_j^{n-1} + \frac{Q_1}{2}(x_{j+1}^{n-1} + x_{j-1}^{n-1})]}{2\Delta t} = \alpha_j^n \tag{5}$$

$$\frac{y_j^{n+1} - [(1-Q_2)y_j^{n-1} + \frac{Q_2}{2}(y_{j+1}^{n-1} + y_{j-1}^{n-1})]}{2\Delta t} = \left(A \frac{\partial y}{\partial r}\right)_j^n + \beta_j^n \tag{6}$$

or in other rewritten form,

$$\frac{x_j^{n+1} - x_j^{n-1}}{2\Delta t} = \alpha_j^n + \frac{Q_1}{4} \frac{\Delta r^2}{\Delta t} \frac{x_{j+1}^{n-1} - 2x_j^{n-1} + x_{j-1}^{n-1}}{\Delta r^2} \quad (7)$$

$$\frac{y_j^{n+1} - y_j^{n-1}}{2\Delta t} = \left(A \frac{\partial y}{\partial r}\right)_j^n + \beta_j^n + \frac{Q_2}{4} \frac{\Delta r^2}{\Delta t} \frac{y_{j+1}^{n-1} - 2y_j^{n-1} + y_{j-1}^{n-1}}{\Delta r^2} \quad (8)$$

It is obvious that $\Delta r \rightarrow 0$ at $\Delta t \rightarrow 0$, so the differential equations obtained by revising equations (7) and (8) are

$$\frac{\partial x}{\partial t} = \alpha + \frac{Q_1}{4} \frac{\Delta r^2}{\Delta t} \frac{\partial^2 x}{\partial r^2} \quad (9)$$

$$\frac{\partial y}{\partial t} = A \frac{\partial y}{\partial r} + \beta + \frac{Q_2}{4} \frac{\Delta r^2}{\Delta t} \frac{\partial^2 y}{\partial r^2} \quad (10)$$

Equations (9) and (10) have the additional artificial viscosity item $v_1 \frac{\partial^2 x}{\partial r^2}$ and $v_2 \frac{\partial^2 y}{\partial r^2}$ compared to their old equations (3) and (4) where

$v_1 = \frac{Q}{4} \cdot \frac{\Delta r^2}{\Delta t}$ and $v_2 = \frac{Q_2}{4} \cdot \frac{\Delta r^2}{\Delta t}$. Their magnitude is closely related to

filtration function Q . v are second-order infinitesimals in case that Q is a first-order infinitesimal, that is, $Q \sim 0(\Delta t, \Delta r)$, they are first-order infinitesimals in case that Q is a zeroth-order infinitesimal, that is, $Q \sim 0(1)$. The filtration function Q is defined as a shape parameter x , the relative fluctuation value of y , that is

$$Q_1 = K_1 \frac{|x_{j+1}^n - 2x_j^n + x_{j-1}^n|}{|x_{j+1}^n + 2x_j^n + x_{j-1}^n|} \quad (11)$$

$$Q_2 = K_2 \frac{|y_{j+1}^n - 2y_j^n + y_{j-1}^n|}{|y_{j+1}^n + 2y_j^n + y_{j-1}^n|} \quad (12)$$

where K_1 and K_2 are constants usually taking values between 0 and 1. Due to the definition of Q , in regions where shape change is wavy the numerators and denominators in equations (11) and (12) may reach the same numerical order at $Q \sim 0(1)$, so the fore-mentioned difference scheme is of first order accuracy. In regions where shape change is smooth, the numerators in equations (11) and (12) are second-order infinitesimals while the denominators are zeroth-order or first-order infinitesimals, so we have at least $Q \sim 0(\Delta t, \Delta r)$, therefore the fore-mentioned difference scheme is of second order accuracy. It is not difficult to prove that this scheme is stable provided the filtration function in difference equations (7) and (8) $Q \in [0, \frac{2}{M} \frac{1}{\Delta r^2}]$. A large number of numerical experiments show that calculation time steps can be enlarged provided the required accuracy is guaranteed. Being compared with previous calculations the time can be reduced by one third in computers along a reentry trajectory.

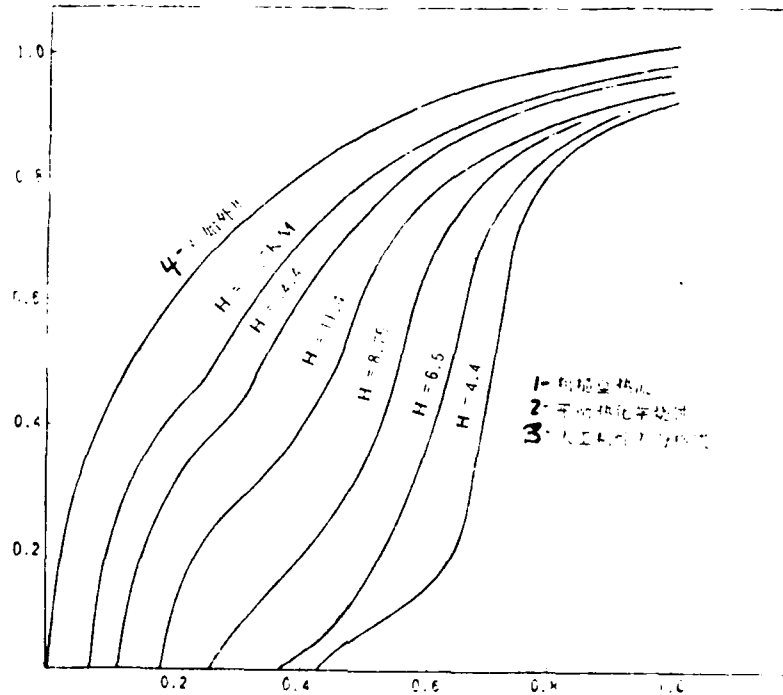
During detailed calculation we have studied the cases of equistep network, changeable step network and changeable time step along x and r directions, respectively. Besides, for comparison we developed several schemes including second difference scheme

smoothed by sampling and first difference scheme smoothed by sampling which are discussed briefly in the next section.

3. Calculation Results and Comparison Analysis

Shape change of ablated reentry nosetip is very significant according to surface roughness of missile nosetip and mechanical erosion of material. Using difference schemes with autocontrol artificial viscosity item to solve ablative shape equations using difference along reentry ballistic, we have successfully calculated the shape upon landing with deep-hollows and long nose cone. Figure 2 shows the time history of ablative shape change obtained by our scheme calculation. Due to this figure the final shape data after autocontrol filtration scheme processing remain smooth and continuous even in the upper region where shape change gradient is significant. It makes ablative shape coupling calculation more simple and concise without necessity of sampling smoothing and evening up. Figure 3 gives shape upon landing calculated by different difference schemes. Comparing the curves in the figure, it can be found that the scheme with artificial viscosity is quite similar to the shape calculated by first order scheme at the upper region because both these schemes are of first order accuracy in this region. The calculated shapes differ significantly from each other in the shoulder region where the two schemes are different in accuracy. Shape (2) is rather close to shape (3) because they are both of second order accuracy. Three schemes yield basically the similar sharp nose cone shape at upper region which means that at upper region surface roughness has a leading effect in controlling shape change while the

effect of diversity of difference schemes on shape calculation is less important.



KEY: 1--rough wall thermal flow; 2--equilibrium thermal chemical ablation; 3--artificial viscosity difference scheme. 4--initial shape.

Figure 2 The history of shape change of ablated nosetip

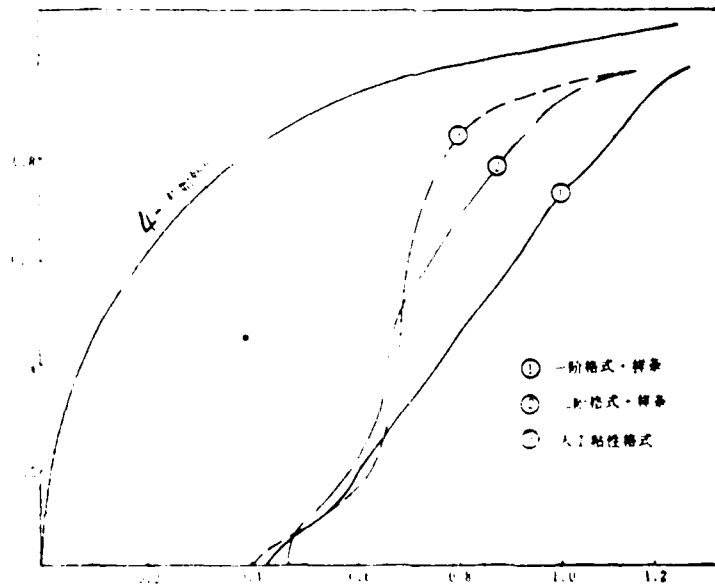


Figure 3 The shape upon landing calculated using different difference schemes

KEY: 1--first order scheme and sampling; 2--second order scheme and sampling; 3--artificial viscosity scheme 4--initial shape

Figure 4 shows effect on shape calculation due to different directions in network calculations. In artificial viscosity scheme, axial equistep network and radial equistep network have little difference in effect on shape calculation, however, radial equistep network can make the calculated points crowding together near stationary point region provided the points before tip shoulder point have the same count. Therefore, when the inflection point moves towards stationary point, prediction becomes more accurate, resulting in more meticulous calculation of pressure and thermal flow near stationary point [3].

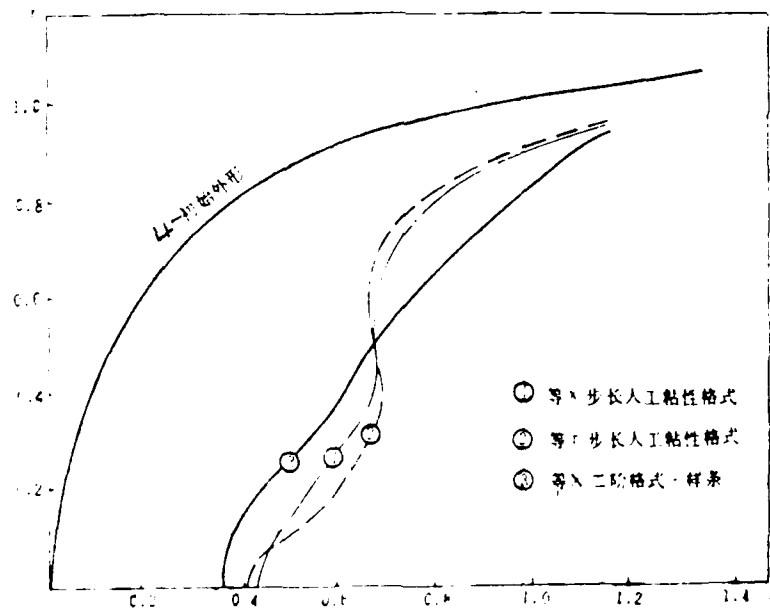


Figure 4 Effects on shape calculation due to different network methods

KEY: 4--initial shape; 1--x equistep artificial viscosity scheme; 2--r equistep artificial viscosity scheme; 3--X equi second order scheme and sampling.

References

- [1] Zhang Hanxing, He Fangshang: Coupling calculation of ablated reentry missile nosetip and aerodynamic characteristics, Technical report No. 002359 of Institute 1705, October 1977.
- [2] Huang Zhenzhong: Spontaneous shape of ablated nosetip and distribution of its inner temperature, <<Acta Aerodynamica>>, No. 1, 1981.
- [3] Yang Maozhao, He Fangshang: A numerical method for engineering of viscosity-free circular fluid of ballistic reentry missile and its surface heating rate, <<Acta Aerodynamica>>. No. 1, 1984.
- [4] Zhang Hanxing et al: A discussion on combined difference scheme, <<The collection of aerodynamic calculation>>, January 1980, pp 111-121.

DISTRIBUTION LIST

DISTRIBUTION DIRECT TO RECIPIENT

<u>ORGANIZATION</u>	<u>MICROFICHE</u>
A205 DMAHTC	1
C509 BALLISTIC RES LAB	1
C510 R&T LABS/AVEADCOM	1
C513 ARRADCOM	1
C535 AVRADCOM/TSARCOM	1
C539 TRASANA	1
C591 FSTC	4
C619 MIA REDSTONE	1
D008 MISC	1
E053 HQ USAF/INET	1
E404 AEDC/DOF	1
E408 AFWL	1
E410 AD/IND	1
F429 SD/IND	1
P005 DOE/ISA/DDI	1
P050 CIA/OCR/ADD/SD	2
AFTT/LDE	1
NOIC/OIC-9	1
CCV	1
MIA/PHS	1
LLYL/CODE L-309	1
NASA/NST-44	1
NSA/T513/IDL	2
ASD/FTD/TQIA	1
FSL	1